Autonomous estimates of horizontal decorrelation lengths for digital elevation models

Andrés Corrada-Emmanuel   Howard Schultz

January 17, 2008

Abstract

The precision errors in a collection of digital elevation models (DEMs) can be estimated in the presence of large but sparse correlations even when no ground truth is known. We demonstrate this by considering the problem of how to estimate the horizontal decorrelation length of DEMs produced by an automatic photogrammetric process that relies on the epipolar constraint equations. The procedure is based on a set of autonomous elevation difference equations recently proposed by Corrada-Emmanuel et al. [5]. In this paper we show that these equations can only estimate the precision errors of DEMs. The accuracy errors are unknowable since there is no ground truth. Furthermore, consideration of the invariance properties of the equations make clear that their application is limited to an imaging sensor that is accurate in its determination of the vertical direction. The practicality of the algorithm for estimating the horizontal decorrelation length of precision errors is shown by application to a set of DEMs produced from images of a desert terrain.

1   Introduction

Research into the geometry of multiple images culminated in the late 1990s with the realization that 3D models of a scene could be created based solely on the images without any knowledge of camera location, orientation or calibration [1, 2]. The correctness of the reconstruction algorithms have been presented qualitatively as in [3] where we are shown a model of a house that looks correct. Or, alternatively, ground truth measurements of the original objects can be compared to their corresponding values in the model as was done by Pollefeys et al. [4]. The faithfulness of these 3D model algorithms raises the question of how far we can extend the autonomy of their verification. Is it possible to create autonomous algorithms that an intelligent sensor could use to verify that it had gathered enough data to reach a prescribed level of correctness? Developing such algorithms would enable a new generation of mapping appliances that could, on their own, explore an environment and reconstruct it without any human intervention. One such algorithm has been presented in [5] where a quantitative estimate of the precision error in the elevation estimates of a Digital Elevation Model (DEM) was presented. This paper will show that a similar precision error computation can be done for the horizontal decorrelation length of DEM postings. This algorithm is also carried out absent any ground truth of the terrain that is being mapped. The limitations of this approach will also become evident when we discuss the invariance properties of the algorithm.

The autonomous estimation of the precision error in 3D model constructions is also related to a second question of general interest. What is the best method for fusing large amounts of information derived from sensors with ever increasing spatial and temporal resolution? Extended image sequences allow us to make multiple models of a scene. How should these different models be fused in an optimal way? Clearly this entails some sort of decision on the relative quality of the models and is therefore intimately related to the precision error estimation presented here.

The paper is organized as follows. The distinction between accuracy and precision is discussed first in the context of DEMs. An idealized version of DEM production process is then introduced that allows us to construct a model for the covariance matrix of precision errors of the elevation estimates in the DEMs. This model is one of many that could be constructed. The ability to compute them autonomously depends on having a large number of DEMs available for comparison and having them be sparsely correlated with each other. The formalism in [5] is then extended to show

how one can compute the variogram of the precision errors and thereby obtain estimates for the horizontal decorrelation lengths of the different DEMs. The horizontal decorrelation length captures the resolution quality of a DEM. It measures the average number of postings between two height measurements such that the elevation errors are decorrelated. The smaller the decorrelation length, the higher the spatial resolution. We measure the horizontal decorrelation length by considering the variogram of the average covariance matrix for the DEM estimates.The limitations of the formalism are then delineated by considering its invariance properties. We conclude by demonstrating the practical utility of the algorithm on a set of ten DEMs of a desert terrain.

2 Geometrical accuracy and precision in 3D model reconstructions

The quality of measurements in scientific fields is discussed using the concepts of accuracy and precision. Accuracy tells us how close an estimate of some physical quantity is to its true value. Precision tells us how many significant digits can be used to quote that estimate. This paper introduces the notions of *geometric accuracy* and *g*eometric precision to understand the errors that occur in 3D reconstructions such as DEMs. These concepts are analogous but not equivalent to the traditional meanings of accuracy and precision.

Consider, for example, the 3D model reconstruction of a garden column in [4]. The column is reconstructed from a sequence of images without any a-priori knowledge of the camera positions, orientations or internal parameters. Comparison with ground truth measurements of landmarks on the column shows that the model is off by a length scale factor of 40.5. However, this scale factor is consistent for all distances between the landmarks with a standard deviation of 5.4% overall. We consider this to be an geometrically inaccurate representation of the column. However, it is a fairly precise reconstruction of the geometry because the scale factor is fairly consistent. Thus it is possible that a 3D model could be wildly inaccurate while being a faithful representation of the shape of the mapped scene.

We can operationalize the distinction between geometric accuracy and precision for 3D models by considering the following procedure. Assume you have a perfect Euclidean model of the scene. Now take the model and apply an arbitrary translation, rotation and scale transformation to it. The model is now geometrically inaccurate but completely precise. This allows one to define a decomposition between accuracy and precision under various global transformations of the data. In particular, precision error can be defined as the infimum of the errors that remain after all possible global transformations are applied to the model to make it overlay on the true scene. Algorithms for calculating this precision error are therefore dependent on the transformations that are allowed. We will show later on that the algorithm presented in [5] is limited to obtaining this geometric precision error when arbitrary translations and rotations parallel to the z-axis are the only allowed transformations.

This distinction between accuracy and precision is analogous to the distinction between bias and variance discussed in the context of regression [6]. Bias tells us how well we reconstruct the true function. Variance tells us how noisy our reconstruction is given the observed data. A well-known decomposition of error in machine learning contexts asserts that errors can be linearly decomposed as the sum of the bias and variance. As we will discuss later in this paper, the geometrical accuracy and precision cannot be so decomposed in general. Therefore, the concepts of geometrical accuracy and precision are not equivalent to bias and variance. The rest of this paper will use the words accuracy and precision to mean geometrica accuracy and precision unless otherwise noted.

This distinction between accuracy and precision in 3D model reconstructions raises the possibility that autonomous precision error estimation is possible while being completely ignorant of the accuracy error of the model. This has practical significance because in many computer vision tasks accuracy is not needed, only precision. For example, if objects in a scene are being detected by shape, one does not care about correctly locating the objects in the world. Resolution, a synonym for precision, should be the goal of the 3D model construction process. Similarly, given a choice between accuracy and precision in a DEM one should prefer precision. Fixing a highly precise DEM could be done with three ground control points. An imprecise but accurate DEM would require one to have many ground control points uniformly spread over the scene. Accuracy is cheaper to fix than precision in some circumstances. Furthermore, by characterizing the precision error of a collection of 3D models one is able to fuse them in a principled way. This fusion based on precision error may create a more precise model at the same time that it increases the accuracy error of the model when compared to the ground truth. For example, the DEM that is most precise may be the most inaccurate.

3 System architecture for precision error estimation in DEMs

The specific algorithm for estimating the precision error of the DEMs that is considered in this paper treats the automatic photogrammetric process that created them as a black box. We assume that we have a collection of DEMs $\{Z_i(x,y)\}$ for $i \in 1, 2, \ldots, n$ that overlap in some local Cartesian plane specified by the coordinates (x, y). One important assumption about this photogrammetric process is that it is based on an epipolar alignment process that uses a dense stereo matcher to compute disparity maps between image pairs. The epipolar alignment of image pairs before stereo matching is a common feature of photogrammetric processes. For our purposes, the important feature of this epipolar alignment step is that it squeezes the error of the stereo matcher to lie along the epipolar lines. This weakens the correlation between the DEMs produced by different image pairs since their epipolar lines will not be parallel. We will assume that these weak correlations are equal to zero.

Another common feature of dense stereo matchers is that they produce asymmetric disparity maps. These asymmetric matches are, for example, used in occlusion detection [7]. The consequence of this asymmetric matching is that the DEM $\{Z_{AB}\}$ produced when matching image A to image B is not the identical to $\{Z_{BA}\}$ produced when B is matched to A. It is assumed in this paper that the photogrammetric process is producing both DEMs and that the labeling of the DEMs allows us to identify such asymmetric pairs. The use of both DEMs may seem troubling since they are, in fact, highly correlated with each other. But as we now discuss, the use of correlated measurements to improve precision is a well-known trick for improving measurements.

4 The importance of keeping both asymmetric DEMs

The use of asymmetric output to improve the performance of a photogrammetric process goes back to Schultz et al. [8]. Comparing asymmetric outputs is a common technique for improving the precision of instruments. Perhaps the best known example is the optical interferometer. In its simplest manifestation it consists of superimposing a forward going beam with a backward going one. The superposition of the waves peaks strongly when the difference in path lengths between the two beams are integral multiples of the beam's wavelength. An interferometer is very precise but potentially very inaccurate as it cannot measure the precise number of wavelengths, just how far we are from an integral number of waves. Besides its use for occlusion detection alluded to before, comparing asymmetries in what are expected to be symmetric outputs is also used to improve the performance of machine translation algorithms [9].

Another good reason for wanting to include asymmetric outputs from a stereo matcher is that it actually gives us the best estimate of the height error at a particular location. Image pairs produce elevation measurements that are not commensurate with each other when projected to the terrain. This is caused by changing geometry of the camera positions but also by the 3D nature of the terrain. Cameras imaging a 2D surface would produce many incommensurate pairs. This effect increases as the surface becomes a 3D object. Thus, the ideal treatment of the data is not to produce a DEM but a DTM with each image pair creating estimates as slightly different (x, y) grids. By using both matches for a pair, we can estimate the error at the same exact spot since we now have two measurements at that spot. The only remaining hurdle in using these two measurements is that they are correlated. But if we can measure this correlation we can then produce a super-resolved DTM with good error estimates.

5 The covariance matrix for the average precision error

The empirical error of a DEM posting at (x, y) is given by $Z_{DEM} - Z_{true} = \delta(x, y)$. The error $\delta(x, y)$ cannot be calculated exactly without some gold standard of elevation measurement that is treated as Z_{true}. We can, however, ask for the average of this error over the whole DEM. In particular, we are interested in the covariance matrix $\langle \delta_i \delta_j \rangle$ of the errors in the elevations for a collection of DEMs.

As argued in [5], this covariance matrix cannot be calculated in general. In other words, it is impossible to solve for the covariance matrix of n measurements without some sort of ground truth. This impossibility is removed if one

focuses on the precision error of sparsely correlated measurements. The basic idea is to consider the set of equations

$$\Delta_{E,M}(x,y) = \frac{1}{E}\sum_{i=1}^{E} Z_i - \frac{1}{M}\sum_{j=1}^{M} Z_j \tag{1}$$

$$= \frac{1}{E}\sum_{i=1}^{E} \delta_i - \frac{1}{M}\sum_{j=1}^{M} \delta_j, \tag{2}$$

where E and M are integers between one and the number of DEMs available. The use of integers for E and M guarantees that, as shown in the second line of equation 1, the unknown value of Z_{true} cancels out exactly for any given posting location. By squaring and averaging all these quantities over all DEM postings, a linear algebra system $Ax = y$ is created for the entries in the average covariance matrix. The vector y is given by the average of the squared difference equations in 1. The vector x represents the average value of the entries in the covariance matrix. This system of linear equations is under-determined in general. The set of equations obtained by squaring 1 has a rank of $\frac{1}{2}n(n-1) - n$ while the average covariance matrix has $\frac{1}{2}n(n-1)$ independent terms. But, as discussed in section 3, the DEM process results in a sparse set of correlations. The average covariance matrix for combining n DEMs therefore requires that we estimate $n + n/2$ terms. This becomes possible whenever three images are available.

When three photographs $\{A, B, C\}$ are available for each DEM posting, the inclusion of asymmetric height estimates results in six height estimates: $\{Z_{AB}, Z_{BA}, Z_{AC}, Z_{CA}, Z_{BC}, Z_{CB}\}$. The standard photogrammetric assumption is that height estimates like Z_{AB} and Z_{AC} are uncorrelated. We retain this simplifying assumption and are led to consider a correlated pair error model of the form

$$\begin{pmatrix} \langle \delta_{AB}^2 \rangle & \langle \delta_{AB}\delta_{BA} \rangle & 0 & 0 & 0 & 0 \\ & \langle \delta_{BA}^2 \rangle & 0 & 0 & 0 & 0 \\ & & \langle \delta_{AC}^2 \rangle & \langle \delta_{AC}\delta_{CA} \rangle & 0 & 0 \\ & & & \langle \delta_{CA}^2 \rangle & 0 & 0 \\ & & & & \langle \delta_{BC}^2 \rangle & \langle \delta_{BC}\delta_{CB} \rangle \\ & & & & & \langle \delta_{CB}^2 \rangle \end{pmatrix} \tag{3}$$

This is to be contrasted with the error model of a system that would not use the asymmetric matches

$$\begin{pmatrix} \langle \delta_{AB}^2 \rangle & 0 & 0 \\ & \langle \delta_{AC}^2 \rangle & 0 \\ & & \langle \delta_{BC}^2 \rangle \end{pmatrix} \tag{4}$$

6 Invariance properties of the autonomous difference equations

The application domain of the autonomous difference equations can be understood by considering the set of transformations that leave them invariant. Clearly any translation along the z-axis causes no change to any of the $\Delta_{E,M}(x,y)$ equations. Likewise, the average of any of the equation remains invariant to x and y translations since it merely reshuffles the postings. Therefore the difference equations are insensitive to translation accuracy errors.

Rotations about any axis parallel to the z-axis also leave the averages of the difference equations invariant. However, any other rotation would project elevation estimates to different (x, y) postings. So strictly speaking, the equations are not invariant to arbitrary rotations. We conclude that the difference equations are only appropriate for an intelligent sensor that has a very good sense of the vertical direction. In practice, DEMs have a horizontal decorrelation length. Rotating the DEMs slightly, say about the x-axis, so that elevation estimates from a given posting do not fall outside this decorrelation length would result in elevation estimates that would have a distribution very similar to the original one. The practical decision of whether this model is applicable to a given collection of DEMs depends on the vertical detection accuracy of the intelligent sensor and the horizontal decorrelation length of the data.

This discussion of the invariance properties of the difference equations should also make clear why the machine learning linear decomposition of error into bias and variance is not applicable to the notions of geometric accuracy and precision. In general, $\{\langle \delta_i \delta_j \rangle\} \neq \{\langle \delta_i \delta_j \rangle\}_{\text{accuracy}} + \{\langle \delta_i \delta_j \rangle\}_{\text{precision}}$ when the precision error is measured with the autonomous difference equations 1.

7 A linear equation system for the variogram of the diagonal entries of the correlated-pair error model

The variogram is a measure of spatial decorrelations of random variables used extensively in geostatistics. For two points $\vec{x}$ and $\vec{y}$ in a spatial process it is defined as $\gamma(\vec{x}, \vec{y}) = 1/2E[(f(\vec{x}) - f(\vec{y}))^2]$. A random variable is said to be *stationary* if its variogram is only dependent on the difference between the points $\vec{x}$ and $\vec{y}$. Additionally, the variable is said to be *isotropic* if its variogram only depends on the distance between two points. We assume in this paper that the DEM precision errors are stationary and isotropic along each of the horizontal plane directions. This allows us to accommodate the case were DEMs could have a higher resolution along one horizontal direction than the other one.

The decorrelation lengths considered here are the ones for the diagonal entries of the correlated-pair error model. For each DEM i, we want to know how its error $\delta_i(x)$ decorrelates with itself. This can be done by calculating the variogram of the error

$$\gamma(\delta_i, L) = \frac{1}{2} \operatorname{E}[(\delta_i(x+L) - \delta_i(x))^2] \tag{5}$$

$$= \operatorname{E}[\delta_i(x)^2] - \operatorname{E}[\delta_i(x) * \delta_i(x+L)], \tag{6}$$

as a function of the lag L between two postings. The first term of the equation above is already known by the linear equation procedure detailed by Corrada et al. [5]. The main contribution of this paper is to show how the same difference equations can be used to calculate the quantities $\operatorname{E}[\delta_i(x) * \delta_i(x+L)]$. Once these are calculated, the decorrelation length can be defined as the horizontal distance L one must move before $\operatorname{E}[\delta_i(x) * \delta_i(x+L)]$ decays to zero.

We proceed by calculating the variogram of the autonomous difference equations 1 as a function of the lag L between postings

$$\gamma_{\mathrm{E,M}}(L) = \frac{1}{2} \operatorname{E}[(\Delta_{E,M}(x+L, y) - \Delta_{E,M}(x, y))^2]. \tag{7}$$

Since the difference equations are linear combinations of the $\delta_i(x)$ for different DEMs $\{i\}$, this equation will contain cross-terms of the form

$$\delta_i(x) * \delta_i(x+L) \tag{8}$$

as desired. In addition, it will contain terms of the form $\delta_i(x) * \delta_j(x+L)$. For DEMs coming from different image pairs, we assume these go to zero under the expectation operation. For DEMs from the same pair, the terms can be collected into single terms of the form

$$1/2 * (\delta_i(x) * \delta_j(x+L) + \delta_i(x+L) * \delta_j(x)). \tag{9}$$

All the terms can then be collected into a linear system of the form

$$\vec{\gamma}(L) = A * \overrightarrow{\operatorname{E}[\delta_i(x) * \delta_j(x)]} - A * \vec{C}, \tag{10}$$

where the matrix A has exactly the same components as those used to solve for the vertical precision errors. The vector $\vec{\gamma}$ has components calculated from the equations 7. It is computed from the observed elevations. The vector $\overrightarrow{\operatorname{E}[\delta_i(x) * \delta_j(x)]}$ are the terms in the correlated-pair covariance matrix. These are computable from the observed elevations also. It is vector $\vec{C}$ that contains the terms (eq. 8) that we want as well as those we are not interested in (eq. 9). Equation 10 can be easily solved for the vector $\vec{C}$ to obtain

$$\vec{C}(L) = \overrightarrow{\operatorname{E}[\delta_i(x) * \delta_j(x)]} - A^{-1}\vec{\gamma}(L), \tag{11}$$

at each lag L. This linear equation can be solved at each lag and then equation 6 can be used to compute the variogram of the precision error for each DEM.

DEM	$< \delta_i^2 >$	$< \delta_i\delta_j > / \sqrt{< \delta_i^2 >< \delta_j^2 >}$	DEM	$< \delta_i^2 >$	$< \delta_i\delta_j > / \sqrt{< \delta_i^2 >< \delta_j^2 >}$
AB	0.050	0.53	AB	0.048	0.50
BA	0.055		BA	0.053	
AC	0.099	0.77	AC	0.054	0.57
CA	0.100		CA	0.054	
AD	0.042	0.46	AD	0.041	0.44
DA	0.036		DA	0.036	
BC	0.117	0.73	BC	0.115	0.73
CB	0.110		CB	0.108	
CD	0.122	0.75	CD	0.104	0.71
DC	0.108		DC	0.089	

(a) Without bias removal. (b) With bias removal.

Table 1: Covariance matrix entries for the ten DEMs in the 29 Palms dataset. Variance is in units of m^2.

8 Bias in geometric precision errors

The asymptotic value of the variogram function for a random variable x as the lag L goes to infinity can easily be shown to be equal to $\text{Var}[x] - \text{E}[x]^2$. Because of this asymptotic behavior, many users of variograms prefer to de-mean their data so that $E[x'] = 0$. A similar consideration is also useful in the context of DEM fusion. A particular DEM may be precise but very different from other DEMs to which it is compared. Calculating the precision error for this DEM would yield a high value in comparison to the other DEMs. Since we are interested in model reconstructions that are precise but possibly inaccurate, this bias in precision should also be removed.

The procedure for removing the bias also uses the autonomous difference equations 1 with $E = N$ and $M = 1$ where N is the total number of DEMs. In this case, we are interested in calculating $\text{E}[\delta_i(x, y)]$ for each DEM. It can be easily shown that the set of equations defined by

$$\left(\frac{1}{N} \sum_{i'=1}^{N} z_{i'}(x, y) \right) - z_i(x, y) = \left(\frac{1}{N} \sum_{i'=1}^{N} \delta_{i'}(x, y) \right) - \delta_i(x, y), \tag{12}$$

also give us a well-determined linear algebra system for calculating this mean precision error bias.

This calculated bias is not an intrisic property of each DEM. The bias is fully dependent on the collection of DEMs that is used to calculate it. Furthermore, application of the bias removal procedure may very well increase the inaccuracy of a final fused DEM while making it more precise.

9 Experimental results

A set of four photographs overlapping on the ground of the Twenty-Nine Palms desert region in California, USA will be used to demonstrate the practicality of this precision error estimation procedure. For ease of discussion we label the photographs as A, B, C, D. The four photographs allow us to create $12 = 4 * 3$ DEMs. We remind the reader that each DEM is the result of matching a pair photographs where reference and target labels matter. The DEM created by matching pixels in photograph A to pixels in photograph B will be denoted by AB. The AB DEM is similar but not equivalent to the BA DEM as discussed in section 4. One DEM pair (BD, DB) was rejected after application of a thresholding step on allowable asymmetric pair differences since all of its postings were identified as blunders. This left 5 pairs or ten DEMs for computation of the variogram of their precision error via equation 11.

The initial results we present are without removing the precision error bias as discussed in section 8. The covariance matrix for the ten DEMs is presented in table 1(a). Note that the {A,C} pair seems to be the worst DEM pair with a cross-correlation of 0.77 when the bias is not removed. Application of the bias removal as detailed in section 8, however, identifies it as comparable to the {A,B} DEM pair. Figure 1 shows the DEMs produced by fusing the DEM pairs together by simple averaging. The best DEM pair {A,D} (figure 1(a)) and the worst DEM pair {B,C}
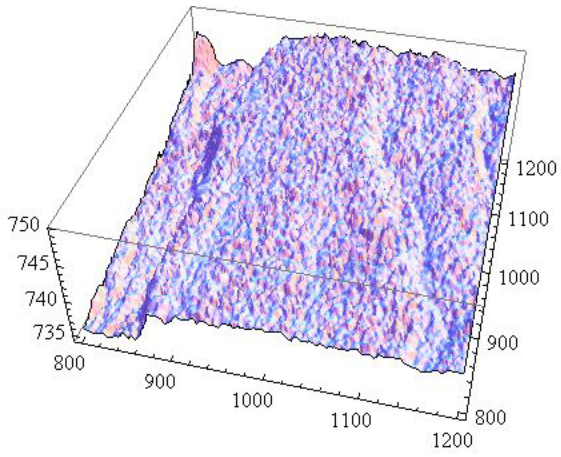
(a) Best pair of DEMs {A,D} fused
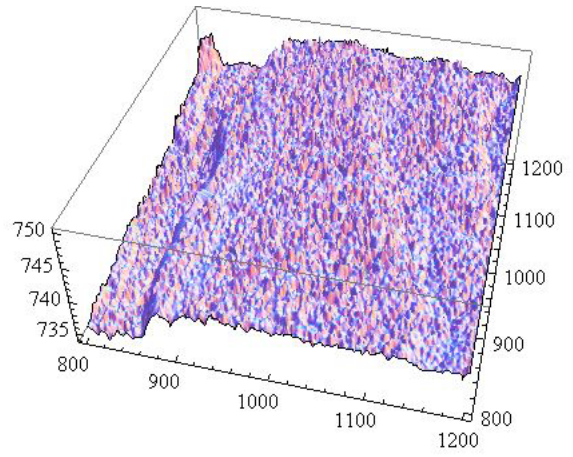
(b) Worst pair of DEMs {B,C} fused
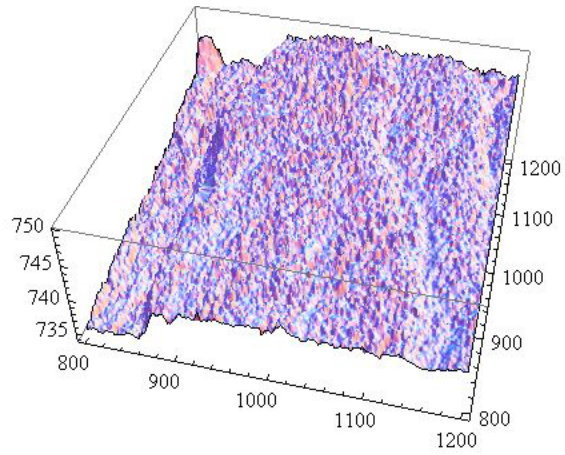
(c) Pair of DEMs {A,C} fused

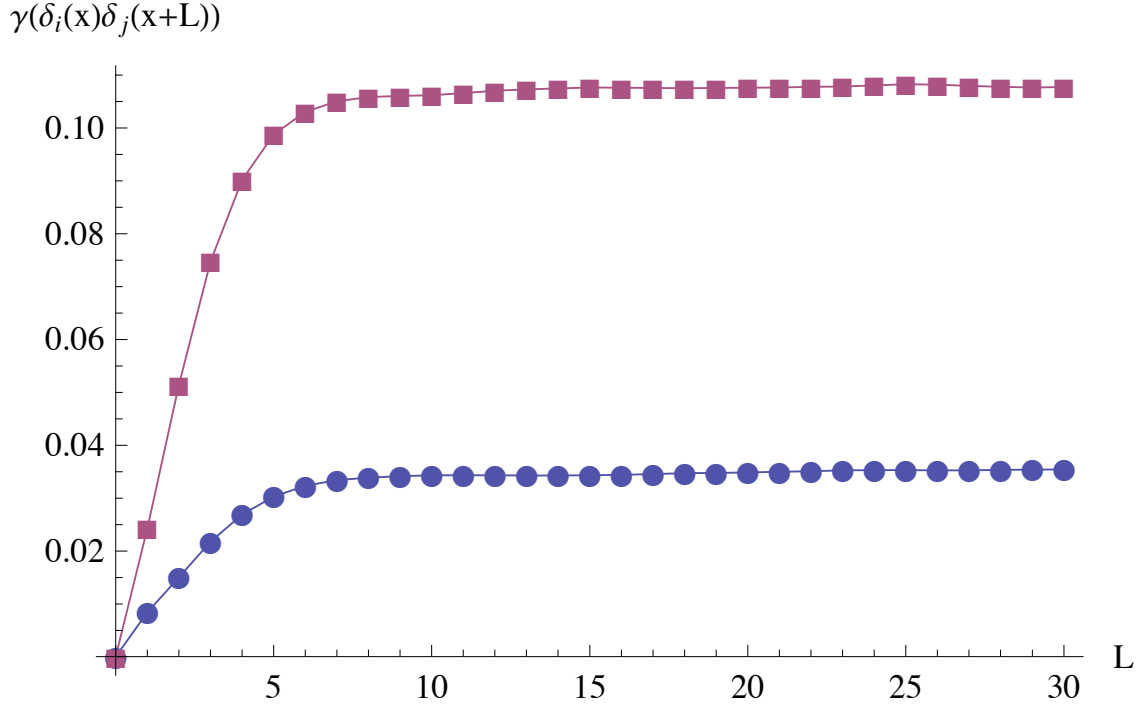Figure 1: A comparison of three fused DEM pairs for a patch of the mapped terrain.

Figure 2: Variograms of two of the ten DEMs after bias. The curve with circle symbols is the most precise with a vertical elevation precision variance of 0.036 m^2. The curve above (square symbol) has a variance of 0.12 m^2. The vertical axis is in units of m^2. The horizontal axis is in units of postings (0.38 meters/posting).

(figure 1(b)) are shown at the top of the figure. The seemingly bad DEM pair {A,C} (figure 1(c)) when the bias is not removed is shown at the bottom for comparison . The quality of the {A,C} pairs does indeed seem to be better than that of the {B,C} pair but worse than that of the {A,D} pair. We take this as evidence for the utility of the bias removal procedure outlined in this paper.

We proceeded to calculate the variograms for the DEMs when the bias has been removed. All variograms behave similarly. The best (DA) and worst (BC) DEMs from table 1(b) are shown in figure 2. The horizontal axis is given in units of postings (each posting is 0.38 meters apart). The variograms are very similar. They both have a decorrelation length of roughly 5 postings or approximately 2 meters. They exhibit the classic shape expected of a spatially correlated random variable that is stationary and isotropic as we have assumed.

Another comparison that can be used to test the validity of the experimental results is to consider the cheating experiment of producing synthetic images from an average DEM. The synthetic images are then fed back into the photogrammetric system and this can then be used to calculate an 'exact' $\delta_i(x)$ for each DEM. Such an experiment was carried out for a similar dataset using an asymmetric pairs photogrammetric system by Schultz et al. [8]. They recovered a horizontal decorrelation length of 2 meters which is comparable to the value calculated here.

Given these decorrelation lengths, we can revisit the question of the applicability of the precision error model considered here to the experimental data. Consideration of the invariance properties of the autonomous difference equations led us to argue that this model is appropriate for an imaging sensor that has an accurate notion of the vertical axis of the terrain. The decorrelation length divided by the vertical height above the terrain gives us an estimate of what this accuracy should be for the present case. The data considered here was posted at distances of 0.38 meters and was imaged at a height of approximately 2,000 meters above the terrain. This results in a desired accuracy of 0.1 degrees or better. This is larger than the accuracy obtainable with GPS/INS instruments that is measured in thousandths of degrees (e.g. Table 3 in [10]).

10 Conclusions and future work

We have shown that horizontal decorrelation length of the precision error in DEMs can be determined with an algorithm that does not know ground truth. Together with the estimates of vertical uncertainty, it is now possible to carry out tuning experiments to detect algorithms and settings that decrease the precision error of a map-making process. This minimization of error may increase the accuracy error but as we have argued, for many machine learning tasks this is not relevant. Since we argue that fixing accuracy is much cheaper than fixing precision, this may be a desirable procedure to follow.

The limitations of the present theory have been amply discussed in our presentation of its assumptions. Nonetheless, we believe it is a good approximation in cases where the horizontal decorrelation length is wide relative to the vertical angle uncertainty of the imaging sensor as argued in the previous section.

The present theory could be extended in various ways. Armed with estimates of the precision error, it now becomes possible to implement autonomous algorithms for the optimal way to fuse photogrammetric data from low-level computer vision tasks such as depth maps.

Future work could also generalize the concept presented in [5] and here to entertain the possibility that DEMs across image pairs could have small but measurable correlations. The sucess of such an approach is dependent on a sufficient number of DEMs so that the correlations remain sparse and the linear system remains well-determined.

Furthermore, we can consider going inside the black box of the photogrammetric system and devise a projective precision error estimation procedure that exploits the group properties of the projective transformations that are used to carry out the epipolar alignment of the images.

Acknowledgements

References

[1] R. Hartley and A. Zisserman, *Multiple view geometry in computer vision*. Cambridge, U.K. ; New York: Cambridge University Press, 2000, richard Hartley, Andrew Zisserman.; Includes bibliographical references (p. 589-599) and index. 1

[2] O. Faugeras, Q.-T. Luong, and T. Papadopoulo, *The geometry of multiple images : the laws that govern the formation of multiple images of a scene and some of their applications*. Cambridge, Mass.: MIT Press, 2001, olivier Faugeras, Quang-Tuan Luong ; with contributions from Th?o Papadopoulo.; Includes bibliographical references (p. [597]-634) and index. 1

[3] P. Beardsley, P. Torr, and A. Zisserman, "3d model acquisition from extended image sequences," in *Part 2 (of 2)*, ser. Proceedings of the 4th European Conference on Computer Vision, ECCV'96, vol. 1065, Cambridge, UK, Apr 1996 1996, p. 683, compilation and indexing terms, Copyright 2007 Elsevier Inc. All rights reserved; T3: Lecture Notes in Computer Science. 1

[4] M. Pollefeys, R. Koch, and L. V. Gool, "Self-calibration and metric reconstruction inspite of varying and unknown intrinsic camera parameters," *International Journal of Computer Vision*, vol. 32, no. 1, pp. 7–25, 1999, compilation and indexing terms, Copyright 2007 Elsevier Inc. All rights reserved. [Online]. Available: http://dx.doi.org/10.1023/A:1008109111715;http://dx.doi.org/10.1023/A:1008109111715 1, 2

[5] A. Corrada-Emmanuel, B. Pinette, A. Ostapchenko, and H. Schultz, "Improving autonomous estimates of dem uncertainties by exploiting computer matching asymmetries," in *8th Conference on Optical 3-D Measurement Techniques*, July 9-12 2007. 1, 2, 3, 5, 9

[6] C. M. Bishop, *Pattern Recognition and Machine Learning*. Springer, 2007. 2

[7] M. Z. Brown, D. Burschka, and G. D. Hager, "Advances in computational stereo," *IEEE Transactions on Pattern Analysis and Machine Intelligence*, vol. 25, no. 8, pp. 993–1008, 2003, compilation and indexing terms, Copyright 2007 Elsevier Inc. All rights reserved. [Online]. Available: http://dx.doi.org/10.1109/TPAMI.2003.1217603;http://dx.doi.org/10.1109/TPAMI.2003.1217603 3

[8] H. Schultz, A. R. Hanson, E. M. Riseman, F. R. Stolle, Z. Zhu, and W. Dong-Min, "A self-consistency technique for fusing 3d information," in *Proceedings of the Fifth International Conference on Information Fusion*, X. R. Li, Ed., vol. 2, 8-11 July, 2002 2002, pp. 1106–1112. 3, 8

[9] R. Zens, E. Matusov, and H. Ney, "Improved word alignment using a symmetric lexicon model," in *COLING '04: Proceedings of the 20th international conference on Computational Linguistics*. Morristown, NJ, USA: Association for Computational Linguistics, 2004, p. 36. [Online]. Available: http://dx.doi.org/10.3115/1220355.1220361 3

[10] M. Cramer and D. Stallmann, "System calibration in direct georeferencing," in *ISPRS Commission III Symposium*, vol. 34. IAPRS, 2002, pp. 79–84. 8